

Manipulating the Local Symmetry and Geometry of Bowtie Optical Antennae for Controlling Spectral Properties while Maintaining the Near-Field enhancement

A. Weber-Bargioni, S. Dhuey, D.F. Ogletree, P.J. Schuck, S. Cabrini
Molecular Foundry, Lawrence Berkeley National Laboratory

Research and Development of plasmonic/optical antennae is a topic of high interest since these antennae enable the manipulation of light in the visible regime on the nm scale ¹. Presently much effort is invested into coupled plasmonic devices since they allow an unprecedented combination of Near Field Optical confinement, enhancement, and control ²⁻⁴. The next R&D phase will be the implementation of well-defined optical antennae into actual devices to employ the novel properties of optical antennae such as localized optical near fields. Important applications are Tip Enhanced Raman Spectroscopy (TERS) ⁵ or Enhanced Raman Spectroscopy incorporated with Nonfluidics, which enables the imaging of single proteins ⁶ and can potentially be used for label-free chemical mapping with a resolution down to individual molecules. The key for the successful device implementation of optical antennae is a) the precise control over their resonances and b) a reproducible fabrication method that allows the incorporation of the antennae into devices that are more complex than just flat substrates.

In this work we present the successful and reproducible fabrication of well-defined functional plasmonic antennae, where we are able to tune the resonance frequency of bowtie antennae by modifying the triangles' aspect ratio or breaking the symmetry of a cross bowtie-like antennae ⁷, all while maintaining the near field enhancement.

We employed e-beam lithography and a novel nanofabrication method termed Induce Deposition Mask Lithography ⁸ (IDML, see figure 1) to reproducibly make Au optical bowtie antennae with specified geometries. The latter allows the flexible placement and implementation of optical antennae into devices such as next generation near-field optical probes, photonic crystals or nanofluidic devices (see figure 2). The resonances of the optical antennae have been determined via dark-field spectroscopy (figure 3) and their resonance frequencies and near field enhancements have been modeled by Finite Element and Finite Difference Time Domain simulation (compare figure 4).

Hence, this work contributes to the fundamental understanding of coupled plasmonic antennae, enabling the specific design, engineering and implementation of optical antennae for particular applications.

1. Crozier, K. B.; Sundaramurthy, A.; Kino, G. S.; Quate, C. F. *Journal of Applied Physics* **2003**, *94*, (7), 4632-4642.
2. Muhlschlegel, P.; Eisler, H. J.; Martin, O. J. F.; Hecht, B.; Pohl, D. W. *Science* **2005**, *308*, (5728), 1607-1609.
3. Schuck, P. J.; Fromm, D. P.; Sundaramurthy, A.; Kino, G. S.; Moerner, W. E. *Physical Review Letters* **2005**, *94*, (1), -.
4. Merlein, J.; Kahl, M.; Zuschlag, A.; Sell, A.; Halm, A.; Boneberg, J.; Leiderer, P.; Leitenstorfer, A.; Bratschitsch, R. *Nature Photonics* **2008**, *2*, (4), 230-233.
5. Stockle, R. M.; Suh, Y. D.; Deckert, V.; Zenobi, R. *Chemical Physics Letters* **2000**, *318*, (1-3), 131-136.
6. Hoppener, C.; Novotny, L. *Nanotechnology* **2008**, *19*, (38), -.
7. Zhang, Z.; Weber-Bargioni, A.; Wu, S. W.; Dhuey, S.; Cabrini, S.; Schuck, P. J. *Nano Letters* **2009**, *9*, (12), 4505-4509.
8. Weber-Bargioni, A.; Schwartzberg, A. M.; Schmidt, M.; Harteneck, B.; Ogletree, D. F.; Schuck, P. J.; Cabrini, S. *Nanotechnology* **accepted**

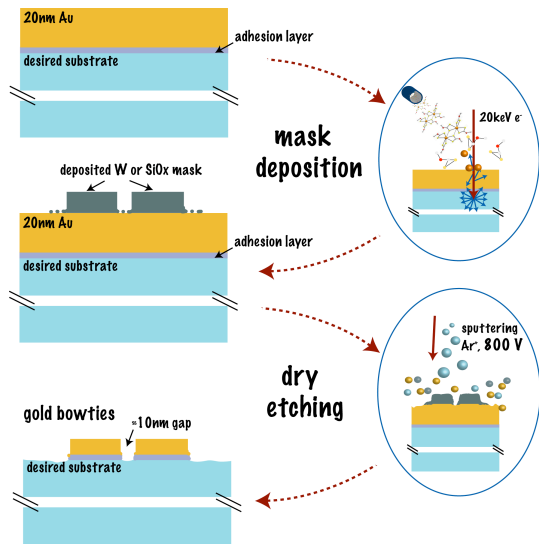


Figure 1 Induced Deposition Mask Lithography method allowing flexible and reproducible implementation of optical antennae into devices

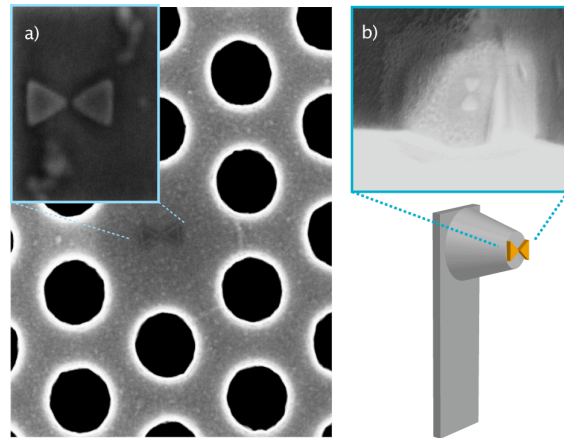


Figure 2 implementation of optical antennae into a) cavity of a photonic crystal b) on the apex of a Scanning Probe tip as next generation Near Field Optical Probe

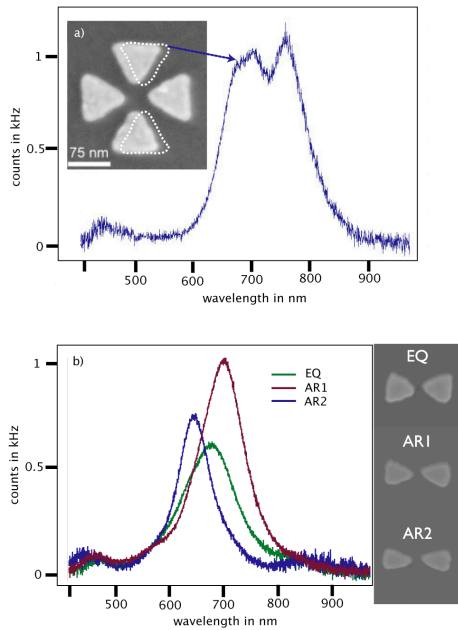


Figure 3 modifying the resonance of optical antennae by a) breaking the symmetry of a cross bowtie antennae leading to a second resonance peak and b) by changing the triangle aspect ratio of a bowtie antenna while keeping the triangle area the same.

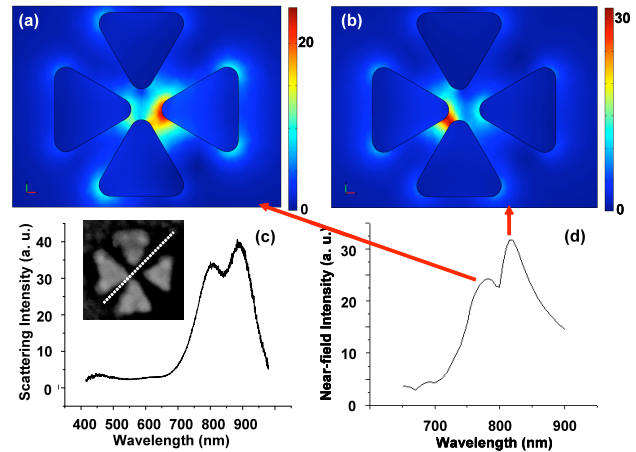


Figure 4 Calculated images of the e-field distributions via FDTD surrounding an asymmetric cross bowtie antenna when excited at (a) 780 nm, and (b) 820 nm. (c) Experimental dark-field scattering spectrum and (d) calculated near-field intensity spectrum from the asymmetric cross antenna. Inset of (c) is an SEM image of the plasmonic antenna from which the scattering spectrum in (c) originated.